Ionization of Li Rydberg atoms by 8.5- and 18-GHz circularly polarized microwave fields

C. H. Cheng, C. Y. Lee, and T. F. Gallagher

Department of Physics, University of Virginia, Charlottesville, Virginia 22901
(Received 3 February 1995; revised manuscript received 24 April 1996)

We have measured separately the ionization threshold fields of the sets of Li states composed of $l+m$ even and $l+m$ odd zero field states. In spite of the fact that the states composed of $l+m$ even states are, by one measure, more nonhydrogenic than those composed of the $l+m$ odd states, we observe that both sets of states ionize at a microwave field well below the hydrogenic ionization field. The ionization of the states composed of $l+m$ odd states shows that even small departures from hydrogen lead to completely nonhydrogenic ionization, as in a static field. In contrast, in a linearly polarized microwave field small departures from hydrogen do not lead to nonhydrogenic ionization. The excitation spectrum of the states composed of $l+m$ odd states exhibits regular structure, while that of the states composed of $l+m$ even states does not, a difference due to the differing energy shifts of $m=0$ and ±1 states on transformation between the laboratory and rotating frames. [S1050-2947(96)09910-6]

PACS number(s): 32.80.Rm

I. INTRODUCTION

Previous work on the microwave ionization of hydrogen and nonhydrogenic atoms by linearly polarized fields shows a striking difference between the two. When the frequency is substantially below the spacing between n states, $\omega \ll 1/n^3$, hydrogen is ionized by a microwave field of amplitude $E \cong 1/9n^4$ [1], while nonhydrogenic atoms can be ionized by a field of amplitude $E \cong 1/3n^5$ [2,3]. Here n is the principal quantum number, and ω is the microwave angular frequency. When units are not given, atomic units are implied. It is possible to see both hydrogenic and nonhydrogenic ionization in the same atom because in a linearly polarized microwave field the azimuthal orbital angular momentum quantum number m remains good, even though n and the orbital angular momentum quantum number l are not good. In Na the $|m|=0$ and 1 states, which include the very nonhydrogenic s and p states with quantum defects of 1.35 and 0.85, are ionized by a 15-GHz field of $E \cong 1/3n^5$ [4]. Ionization occurs by transitions to higher-lying states by partially diabatic traversals of the avoided Stark level crossings in the time varying field, followed by ionization when it becomes possible. The magnitude of the avoided crossings is roughly proportional to the quantum defect of the lowest l state of the m states under study. In light of this fact it is not so surprising that the $|m|=2$ states, which have the d states of quantum defect 0.015 as their most nonhydrogenic constituent, are ionized by a 15-GHz field of $E=1/9n^4$ [4]. The $|m|=2$ avoided level crossings are so small that they are traversed purely diabatically, and microwave ionization occurs as in H, by field ionization of the initially populated n state.

Classically the Δn transitions at the avoided crossings of $|m|=0$ and 1 states correspond to the Rydberg electron's scattering into a qualitatively different orbit of the same energy when it comes near the Na$^+$ core. In H such scattering into very different orbits does not occur, and in the Na $|m|=2$ states the electron does not come close enough to the Na$^+$ core to sense that it is not a point charge but has a finite size.

The fact that for linear polarization there exists such clear evidence for hydrogenic and nonhydrogenic microwave ionization in the same atom suggests that the same might be true for a circularly polarized microwave field. Recent experiments in Na have shown that at frequencies of ~10 GHz a field amplitude of $E=1/16n^4$ is required for ionization [5], while in H the required field is $E \cong 1/6n^4$ [6,7], in agreement with a recent calculation by Rakovic and Chu [8]. In a circularly polarized field none of the n, l, and m quantum numbers is good, and the axis of quantization coincides with the axis about which the field rotates. However, due to the $\Delta l=\pm1$, $\Delta m=\pm1$ dipole selection rule in a circularly polarized field there are two distinct sets of states, one composed of linear combinations of zero field states of $l+m$ even, and one composed of linear combinations of zero field states of $l+m$ odd. For simplicity we shall refer to these sets of states as the $l+m$ even states and $l+m$ odd states. Although the labels are derived from the zero field compositions of the states, it must be borne in mind that in a nonzero field neither l nor m is a good quantum number.

In Li the s, p, and d states have quantum defects of 0.399, 0.053, and 0.002, respectively, so only the s and p states have quantum defects larger than the Na d state quantum defect. Consider how the states of quantum defect $>10^{-2}$ are distributed. The $l+m$ even states have the s state and the p $m=\pm1$ states spread over $n^2/2$ states, while the $l+m$ odd states have only the p $m=0$ state spread over $n^2/2$ states. In the latter case the dilution of the nonhydrogenic state is clearly greater than it is for the Na d $m=\pm2$ states which are each spread over $n-2$ states. In more physical terms, in the $l+m$ even states the Rydberg electron can come closer to the Li$^+$ core than in the $l+m$ odd states. On average, the Li $l+m$ odd states ought to be considerably more hydrogenic than the $l+m$ even states, and it is conceivable that the Li $l+m$ odd states might ionize at the hydrogenic ionization field while the $l+m$ even states ionize at the lower field required by Na.

Here we report the measurements of ionization of the Li $l+m$ even and odd states, by 8.5- and 18-GHz circularly polarized microwave fields. In the following sections we describe the experimental approach, present the results, which
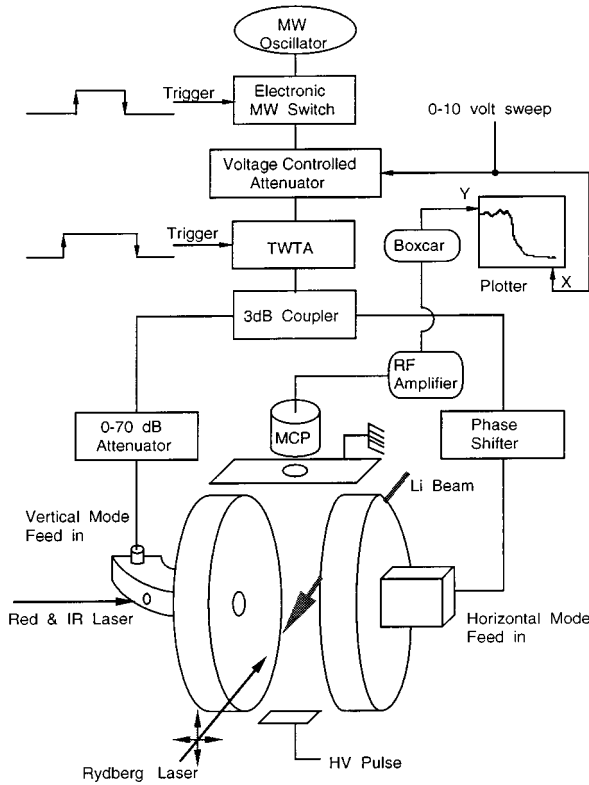
FIG. 1. Schematic diagram of the experimental apparatus.

are in all cases similar to those obtained in Na, and discuss the implications of our observations.

II. EXPERIMENTAL METHOD

The approach used in these measurements is similar to that employed by Fu *et al.* [5] and Lee *et al.* [9]. As shown by Fig. 1, Li atoms in a thermal beam pass through a Fabry-Perot microwave cavity where they are excited to Rydberg states in the presence of the circularly polarized microwave field by pulsed dye lasers running at a 20-Hz repetition rate. The atoms are excited by the route

$$2s \xrightarrow{671 \text{ nm}} 2p \xrightarrow{813 \text{ nm}} 3s \xrightarrow{620 \text{ nm}} np \qquad (1)$$

using three pulsed dye lasers. The last laser is polarized parallel or perpendicular to the symmetry axis of the cavity, about which the microwave field rotates. With parallel polarization $l+m$ odd states are excited, via their np $m=0$ components, and with perpendicular polarization $l+m$ even states are excited, via their np $m=\pm1$ components. As shown by Fig. 1, the laser beams cross in the center of the cavity, producing a volume of excited atoms about 1 mm on a side. The microwaves are turned off 800 ns after the laser pulse and a high voltage pulse applied to the plate below the cavity. This pulse produces a field of 10–30 V/cm at the center of the cavity, which is adequate to expel ions produced by microwave ionization from the cavity but not to ionize the states under study. A static field of this size cannot be present during the microwave pulse for it dramatically alters the ionization [9]. We detect the ions with a microchannel plate detector and capture the resulting signal with a

TABLE I. The parameters of two different Fabry-Pérot cavities.

resonant frequency	8.50 GHz	18.0 GHz
resonant mode	TEM$_{002}$	TEM$_{006}$
Q_H (coupling)	2192 (100%)	2865 (97%)
Q_V (coupling)	1840 (99%)	3582 (66%)
R, curvature of mirrors	15.88 cm	10.20 cm
D, mirror separation	5.79 cm	6.14 cm
H, radius of mirrors	5.50 cm	4.05 cm
d, diameter of irises	0.93 cm	0.50 cm
Γ, geometric factor	0.8104	0.7844

gated integrator. The integrator signal is recorded as the microwave power or the wavelength of the laser is swept.

We produce the circularly polarized field in the cavity by setting up two orthogonally linearly polarized standing waves of the same amplitude but 90° out of phase. The microwave power comes from a Hewlett Packard (HP) 8350B sweep oscillator with an 83550A 8–20-GHz plug in. The microwaves pass through a General Microwave FM 8628 switch which forms 1-μs-long pulses at a 20-Hz repetition rate. The microwaves then pass through a Triangle Microwave 2-gt-41 voltage controlled attenuator before being amplified by a Litton 624 100-W amplifier for the 8.5-GHz measurements or a Hughes 1277H 20-W amplifier for the 18-GHz measurements. After the amplifier the power is split into two arms for the two polarizations by a 3-dB waveguide directional coupler. In one arm there is a HP X885A or P885A phase shifter, and in the other a HP X382A or P382A precision variable attenuator. Both arms have 20-dB directional couplers, to allow power measurement with a HP 432A power meter, and circulators at the vacuum wall to allow detection of the reflected power. Beyond the vacuum wall the power is transported by coaxial cable to short pieces of waveguide attached to the cavity mirrors. As indicated in Fig. 1, the two waveguides are oriented orthogonally to each other and couple orthogonally polarized fields into the cavity through irises in the two mirrors.

The cavities are made of brass, and the parameters of the 8.5- and 18-GHz cavities are given in Table I. Note that the frequencies of the two polarization modes differ by less than their linewidths and the Q's of the vertically and horizontally polarized modes, Q_V and Q_H, are not the same. The latter implies that, while we can produce a circularly polarized field in steady state, the field is not circularly polarized as the field turns on and off. The field distribution of a linearly polarized field inside the cavity is a Gaussian TEM$_{00q}$ mode described by [10,11]

$$E(r,z,t) = \frac{E_0 w_0}{w(z)} \cos\omega t \; e^{-2r^2/w^2(x)}$$
$$\times \cos\left(kz - \Phi(z) + \frac{kr^2}{2R(z)}\right), \qquad (2)$$

where E_0 is the field amplitude at the center of the cavity, i.e., at $z=0$ and $r=0$, z being the distance measured along the cavity symmetry axis and r being the distance from the symmetry axis. The wave number $k=2\pi/\lambda$, where λ is the

free space wavelength. The waist $w(z)$, radius of wavefront curvature $R(z)$, and phase shift $\Phi(z)$ from a plane wave are given by

$$w(z) = w_0 \left[1 + \left(\frac{\lambda z}{\pi w_0^2} \right)^2 \right]^{1/2}, \qquad (3a)$$

$$R(z) = z \left[1 + \frac{\pi w_0^2}{\lambda z} \right], \qquad (3b)$$

and

$$\Phi(z) = \tan^{-1} \left[\frac{\lambda z}{\pi w_0^2} \right]. \qquad (3c)$$

The waist at the center of the cavity is given by

$$w_0^2 = \frac{\lambda}{2\pi} \left[D(2R - D) \right]^{1/2}, \qquad (4)$$

where R is the radius of curvature of the mirrors and D is their separation on the cavity axis. The resonance condition is

$$kD - 2\Phi(D/2) = (1 + q)\pi. \qquad (5)$$

An important point to note about Eq. (2) is that the magnitude of the field is axially symmetric and does not depend on the polarization. Thus, if the field is circularly polarized at one point in the cavity it is circularly polarized at all points. As shown by Eq. (2), the spatial variation of the field is on the scale of the microwave wavelength, several cm, so the field variation over the sample of excited atoms is less than 1%.

In MKS units the field amplitude E_0 of Eq. (2) is related to the input power to the cavity by

$$E_0 = \left(\frac{4PQ}{\pi^2 \epsilon_0 f_0 \Gamma D w_0^2} \right)^{1/2}, \qquad (6)$$

where f_0 is the cavity frequency, Γ is a geometrical factor of order 1, and ϵ_0 is the permittivity of free space, 8.85×10^{-12} F/m. The power P in Eq. (6) is the power required to produce a linearly polarized field of amplitude E_0. To produce a circularly polarized field of the same amplitude requires this power in each of the two modes and thus twice the power specified in Eq. (6). For the low Q arms of the 8.5- and 18-GHz cavities 1 W of input power produces linearly polarized fields of 157 and 246 V/cm, respectively. We estimate that we are able to measure the fields in the cavity with an uncertainty of 12%. As a consistency check we have verified that the linear polarization Li microwave ionization thresholds obtained using this calibration procedure agree with previous measurements using rectangular cavities [12]. Specifically, for $32 \leq n \leq 36$ we have verified that our 8.5-GHz threshold fields typically differ from the previous 8-GHz measurements by 4% and never by more than 10%. For $23 \leq n \leq 29$ our 18-GHz threshold fields are within 8% of the previous 15-GHz measurements.

To set the 0–70-dB attenuator and phase shifter shown in Fig. 1 so as to produce a circularly polarized field we first set the amplitudes of the two field modes to the same value by
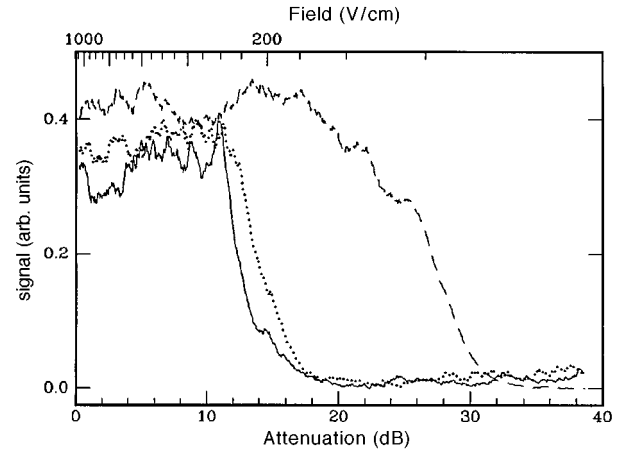

FIG. 2. Ionization signals obtained while exciting the Li atoms to the energy of the zero field $32p$ state: linearly polarized 8.5-GHz microwave field, $m = 0$ (---); circularly polarized microwave field, $l + m$ even ($\cdots$); and circularly polarized microwave field $l + m$ odd (—).

adjusting the 0–70-dB attenuator in the arm feeding the vertically polarized mode so that ionization by either the field of the vertically or horizontally polarized mode alone occurs at the same attenuation of the voltage controlled attenuator. Then, with both field modes present and having the same amplitude, above the threshold for ionization by a linearly polarized field, we adjust the phase shifter in the arm feeding the horizontally polarized mode to minimize the ionization signal. When the field is far above the threshold for linear polarization ionization, but below that for ionization by a circularly polarized field, there is a sharp dip in the ionization signal at the correct phase for circular polarization. At this point small iterative adjustments to the attenuator and phase shifter lead to the closest approximation to circular polarization. We estimate that the two modes have amplitudes which differ by less than 6%, a phase shift which differs from 90° by less than 1°, and an angle between the two polarization axes which differs from 90° by less than 0.4°.

The timing sequence is as follows. A 1-μs microwave pulse is injected into the cavity, and 200 ns after its start the 5-ns laser pulses arrive, so the atoms are exposed to the microwave field for 800 ns. Approximately 200 ns after the microwaves are turned off an 800-ns risetime high voltage pulse is applied to the lower plate to drive any ions produced to the microchannel plate detector. The entire process is repeated at the 20-Hz repetition rate of the lasers. The detector signal is captured by a gated integrator, the averaged output of which is recorded on an x-y recorder.

III. OBSERVATIONS

We measured the ionization signal as the amplitude of the microwave field was varied with the voltage controlled attenuator. In Fig. 2 we show typical traces, obtained at 8.5 GHz with both linearly and circularly polarized microwaves with the final laser set to the wavelength which would excite the Li $32p$ state in zero field. In the presence of either a linearly or circularly polarized microwave field many states fall within the bandwidth of the laser. With a linearly polarized microwave field and the third laser polarized to excite

TABLE II. The measured 8.5-GHz circularly polarized microwave ionization threshold fields at the energies of the Li $n_{mw}p$ states. The uncertainty in the threshold fields is $\pm15\%$.

n_{mw}	$l+m=$odd E_{th} (V/cm)	$l+m=$even E_{th} (V/cm)
25	768	635
26	662	604
27	532	498
28	450	438
29	406	359
30	342	300
31	292	261
32	250	224
33	222	198
34	198	158
35	164	141
36	151	141
37	137	131
38	121	118
39	114	108
40	101	96.7
41	93.3	88.1
42	79.9	77.7
43	75.0	71.5
44	67.4	64.9
45	60.3	58.3
46	54.1	52.5
47	49.2	49.2
48	42.9	43.2
49	40.9	39.7
50	37.4	35.6
51	31.7	31.6
52	26.6	27.4
53	25.8	25.6
54	21.9	23.5

TABLE III. The measured 18-GHz circularly polarized microwave ionization threshold fields at the energies of the Li $n_{mw}p$ states. The uncertainty in the threshold fields is $\pm15\%$.

n_{mw}	$l+m=$odd E_{th} (V/cm)	$l+m=$even E_{th} (V/cm)
32	297	252
33	238	214
34	244	192
35	191	167
36	160	151
37	154	136
38	128	114
39	141	104
40	109	104
41	91.3	88.8
42	76.3	73.9
43	76.3	72.7
44	91.9	66.0
45	52.8	52.1
46	48.3	45.6
47	40.9	40.9
48	38.3	36.4
49	31.7	33.2
50	27.2	26.2
51	27.1	26.6
52	27.1	25.8
53	24.5	22.2
54	16.6	16.5
55	12.2	13.1

the p $m=0$ components of states at this energy we observed 50% ionization at a field of 42.4 V/cm, as shown in Fig. 2. We define the field at which 50% ionization occurs as the threshold field. For the third laser polarized so as to excite $m=\pm1$ states the threshold field is virtually the same, so the data are not shown. With a circularly polarized microwave field and the third laser polarized to excite either $l+m$ even or $l+m$ odd states the thresholds occur at much higher fields than for linear polarization. In addition, it is evident that the $l+m$ odd states, the more hydrogenic ones, have a slightly higher threshold field than the $l+m$ even ones. Most of the apparent structure at microwave fields above the threshold fields is due to laser intensity fluctuations and is not reproducible, the exception being the peaks appearing in the first 100 V/cm above the threshold field in the $l+m$ odd trace, having an origin we shall discuss later. In all cases using several traces we are able to determine the threshold fields to $\pm2.3\%$, and we assign an uncertainty, including the field calibration, of $\pm15\%$ to our threshold fields.

The measurements shown in Fig. 2 have been carried out over a range of states. In all cases the third laser was tuned to the energy of a zero field np state, since this choice of en-

ergy is easily reproduced in another experiment. As noted above, in the presence of a microwave field we usually excite more than one state, all of which have the same energy, and what we observe is the ionization field as a function of binding energy relative to the zero field limit. However, field ionization and microwave ionization fields have most often been described as functions of principal quantum number, not as functions of binding energy. To follow the convention of using the principal quantum number while reminding the reader that we are not exciting a single state, we introduce a nominal principal quantum number n_{mw}, which is defined as follows. The ionization field associated with n_{mw} is the ionization field observed with the laser tuned to the excitation energy of the zero field $n_{mw}p$ state. We present the 50% ionization threshold fields vs n_{mw} in Tables II and III for 8.5 and 18 GHz, respectively. A more illuminating way of presenting the results of Tables II and III is Fig. 3, a logarithmic plot of the threshold fields vs n_{mw}. All the data lie slightly below $E=1/16n_{mw}^4$, as is the case for Na, and none of the data lie near the hydrogenic ionization field of $E=1/6n^4$. However, there is a discernable difference between the $l+m$ even and $l+m$ odd states. At low n_{mw} the $l+m$ even states are ionized at lower fields than the $l+m$ odd states. In Fig. 3 it is also apparent that the ionization fields fall further below $E=1/16n_{mw}^4$ as n_{mw} is increased, and that this phenomenon is more pronounced at 18 than 8.5 GHz, as in Na.

Although the ionization of the $l+m$ even and $l+m$ odd states is not particularly different, their excitation spectra in
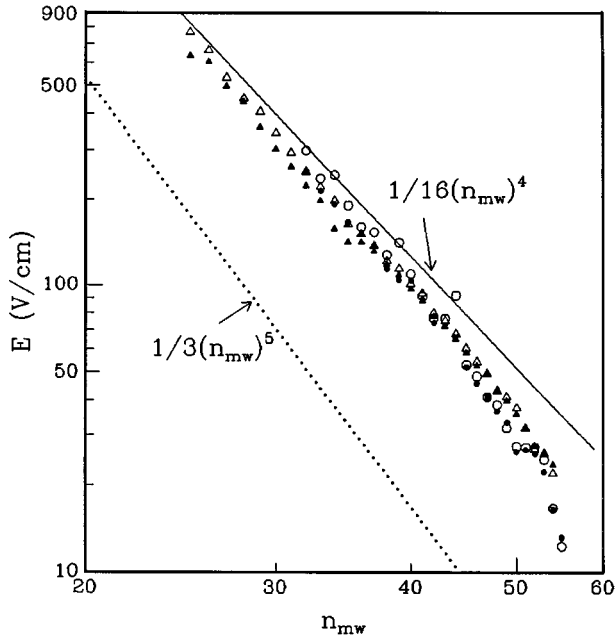
FIG. 3. Measured 50% ionization threshold fields vs n_{mw} for Li at 8.5 and 18 GHz; 8.5 GHz, $l+m$ odd ($\triangle$); 8.5 GHz, $l+m$ even ($\blacktriangle$); 18 GHz, $l+m$ odd ($\bigcirc$); and 18 GHz, $l+m$ even ($\bullet$).

the presence of the circularly polarized microwave field exhibit a pronounced difference, as shown in Fig. 4. Excitation of the $l+m$ odd states, obtained with the third laser polarized parallel to the cavity axis, leads to the spectrum of Fig. 4(a). There is no signal below the threshold for ionization, at a binding energy of 175 cm^{-1}, and oscillatory structure above it. With the third laser polarized perpendicular to the cavity axis to excite $l+m$ even states we obtain the spectrum of Fig. 4(b), in which no regular structure is evident. The origin of the structure of Fig. 4(a) becomes apparent when we compute the energy levels in a frame rotating with the 8.5-GHz rotating field. We have used an adaptation of the matrix diagonalization method of Zimmerman *et al.* [13]. Briefly, the known energies of the zero field nlm states specify their Coulomb wave functions, which are used to calculate electric dipole matrix elements between states differing in l and m by 1. This procedure gives matrix elements with a fractional accuracy of 2.5×10^{-6}. The zero field energies of the states in the rotating frame are obtained by adding $-m\omega$ to their energies in the laboratory frame. Using these energies and dipole matrix elements, a truncated Hamiltonian matrix is then diagonalized to find the eigenvalues and eigenvectors in the rotating frame for different values of the field. As the field is raised the levels exhibit Stark shifts roughly analogous to those observed with a static field. Since $l+m$ even and odd states are decoupled from each other we diagonalize the two matrices separately. The number of basis states required to obtain accurate results depends on the field strength. To find the $n_{mw} \cong 26$ energy levels in a field of 790 V/cm we have carried out the diagonalizations with basis sets of different sizes, including the states of $25 \leq n \leq 27$, $24 \leq n \leq 28$, and $23 \leq n \leq 29$. The maximum change in the energy of a state is 0.51 cm^{-1} when the number of n manifolds included is raised from three to five, and the maximum change falls to 0.22 cm^{-1} as the number of n manifolds is raised from five
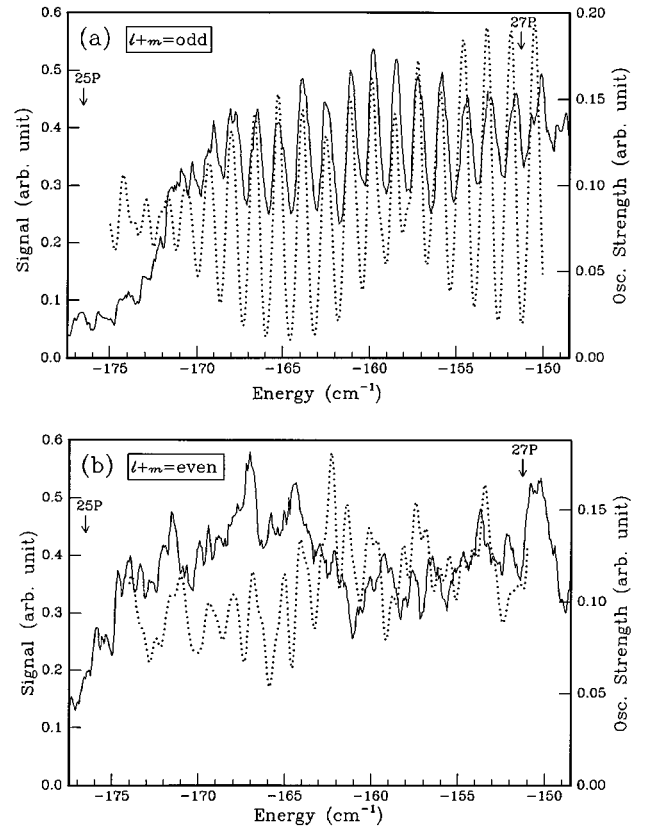

FIG. 4. Excitation spectra in a 790 V/cm 8.5-GHz circularly polarized field (a) $l+m$ odd, experimental trace (——), calculated spectrum ($\cdots\cdots$); (b) $l+m$ even, experimental trace (——), calculated spectrum ($\cdots\cdots$). The arrows show the location of the zero field $25p$ and $27p$ states in both cases.

to seven. Unfortunately, computer limitations do not allow us to do the diagonalizations with nine n manifolds. Nonetheless, several considerations suggest that seven n manifolds are adequate for our purposes. First, using the first-order expression of Wintgen [14] we find that less than 1% of the $n=30$ states shift to the energy range of interest, $n_{mw} \cong 26$, at 790 V/cm. Second, the progression from three to seven n manifolds suggests that the energies computed with seven n manifolds are accurate to 0.2 cm^{-1}. Finally, and most important, the qualitative appearance of the energy level diagram is unchanged as the number of manifolds included in the calculation is increased from five to seven.

Using seven n manifolds we obtain the energy level plot of Fig. 5 for $l+m$ odd, and the $l+m$ even plot is practically identical. In Fig. 5 there are two generic classes of states. First, the levels emanating from the zero field $n=26$ levels are grouped together into energy bands of diabatic states, which are quite evident in Fig. 5. Second, those states emanating from zero field $n \neq 26$ states have very large Stark shifts. In zero field the $n=26$ bands are 0.28 cm^{-1} apart, the microwave frequency, and as the field is increased the spacing between the bands increases, due to the Stark coupling of the levels. At the field of 790 V/cm, the field at which the spectra of Fig. 4 were taken, the spacing between the $n=26$ bands is 1.35 cm^{-1}, corresponding to the spacing of the oscillations in Fig. 4(a). The levels diabatically connected to zero field levels of $n \neq 26$ contribute about 20% of the oscil-
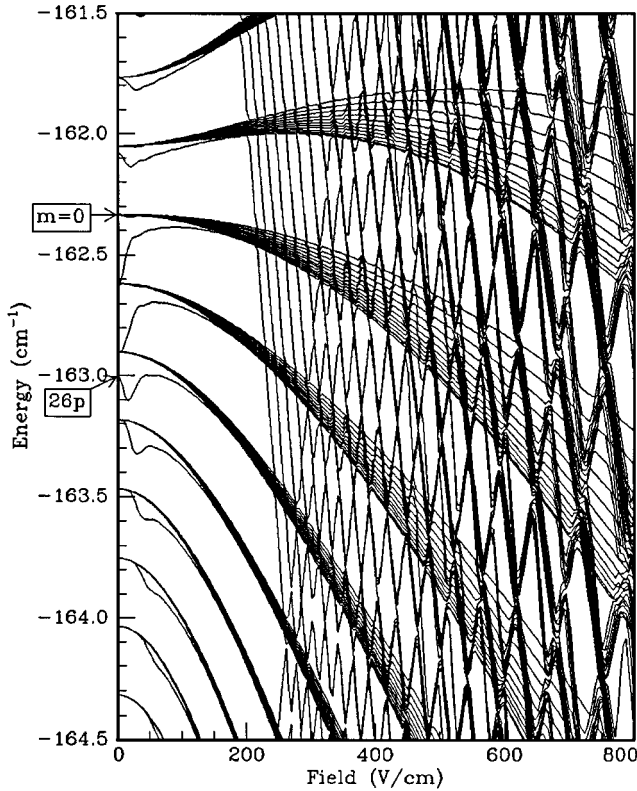
FIG. 5. Calculated Li $l+m$ odd energy levels as a function of field for a field rotating at a frequency of 8.5 GHz. The energy levels are in the rotating frame and are computed by diagonalization of a matrix containing $l+m$ odd states of $n=23$ to 29. It is evident that the levels adiabatically connected to zero field $n=26$ levels lie in the bands which are 8.5 GHz apart in zero field.

lator strength and have such steep slopes that they are unresolvable with our laser resolution and lead to only a small, approximately constant background signal in Fig. 4.

The energy level diagram of Fig. 5 suggests that it is possible that the structure in the $l+m$ odd spectrum of Fig. 4(a) arises from the bands of states coming from the zero field $n=26$ states. To test this notion quantitatively, it is necessary to compute the oscillator strength distributions, i.e., the distribution of p character. For fields near the ionization fields the s and p states are found to be uniformly distributed over the levels in the field. Consequently, the ionization rates of all the states at a given energy can be expected to be comparable. We can calculate the oscillator strength for comparison to Fig. 4 in the following way. The np $m=0$ amplitudes in each eigenstate are weighted by $1/n^{3/2}$ and added, yielding the total p excitation amplitude of the eigenstate. Squaring this amplitude gives the oscillator strength (to within a constant factor). Not surprisingly, for energies near the zero field $n=26$ energy, i.e., $n_{\mathrm{mw}}=26$, the dominant contributions to the oscillator strengths come from the $25p$, $26p$, and $27p$ states, and the contributions from the $29p$ state are less than 10% of those of the $26p$ state. Since the contributions from higher-lying states must be smaller, it is a reasonable approximation to ignore them. We note that we have computed the oscillator strengths in the rotating frame, but for $m=0$ the energies are the same in both the rotating and laboratory frames so we may use the rotating

frame oscillator strengths with no corrections to compute the spectrum.

Once the oscillator strengths of all the levels are determined, their spectrum is convoluted with the laser bandwidth, 0.57 cm^{-1} FWHM, to give the computed spectrum shown by the dotted line of Fig. 4(a). As shown by Fig. 4(a) both the calculated and experimental spectra contain oscillations with the same frequency and phase, suggesting that the bands of $n=26$ states seen in Fig. 5 are indeed the origin of the oscillations in Fig. 4(a). At the highest energies of Fig. 4(a) the observed amplitude of oscillation decreases whereas the calculated amplitude is a maximum. This discrepancy can be explained as follows. With increasing energy the number of overlapping n manifolds, with different band spacings, increases, hence the observed diminution of the amplitude of the oscillations. Due to our truncation of the Hamiltonian matrix, as the energy approaches the $n=29$ energy, -130 cm^{-1}, in our calculation the number of overlapping n manifolds decreases leading to an increase in the amplitude of the calculated oscillations. We attribute the structure at fields above the ionization threshold in the $l+m$ odd trace of Fig. 2 to the shifts of the energies of the peaks in spectra such as the one shown in Fig. 4(a) with microwave power.

The spectrum of the $l+m$ even states, shown in Fig. 4(b), is computed in the same way. As noted above, for the $l+m$ even states the energy level diagram is virtually identical to Fig. 5. Furthermore, when the rotating frame oscillator strengths to the np $m=\pm1$ states are computed, as outlined above, most of the oscillator strength is again found in bands of states 1.35 cm^{-1} apart. Why, then, is there no regular structure in Fig. 4(b)? The answer is the transformation to the laboratory frame. When an $m=\pm1$ state is transformed to the laboratory frame, its energy is shifted by $\pm\omega$, which is ±8.5 GHz in this case. Thus each of the bands of oscillator strengths in the rotating frame is split into two bands separated by 17 GHz in the laboratory frame. When this oscillator strength is convoluted with the laser linewidth, the amplitude of the oscillations in the spectrum is substantially diminished, as shown in the calculated spectrum of Fig. 4(b).

IV. CONCLUSION

This work shows clearly that the ionization of Li by 800-ns pulses of a circularly polarized microwave field is not hydrogenic for either $l+m$ even or $l+m$ odd states, in spite of the fact that the latter states are more hydrogenic. However, we suspect that ionization field measurements with shorter microwave pulses or measurements of ionization rates would reveal a difference. In addition, this work underscores the difference between ionization by linearly and circularly polarized microwave fields. Why are these two microwave ionization processes so different? In both cases the interaction of the Rydberg electron with the finite-sized core is important. Quantum mechanically, a linearly polarized field couples a state to higher-energy states of the same m, which must be low if the states in question are populated by purely optical means. Since all the coupled states have the same low m, the core coupling is relatively strong. In contrast, a circularly polarized field couples a state to states of higher energy with higher m (or lower m if the sense of

polarization is reversed). As a result, an optically excited state of low m is only coupled to higher energy states of higher $|m|$, reducing the core interaction. From a classical point of view, in a linearly polarized field the electron can scatter repeatedly from the core as it gains energy, but in a circularly polarized field the likelihood of scattering from the core decreases as the electron gains energy from the microwave field. From either the classical or quantum-mechanical point of view it is not surprising that microwave ionization occurs at lower fields with linear rather than circular polarization.

[1] J. E. Bayfield and P. M. Koch, Phys. Rev. Lett. **33**, 258 (1974).

[2] P. Pillet, W. W. Smith, R. Kachru, N. H. Tran, and T. F. Gallagher, Phys. Rev. Lett. **50**, 1042 (1983).

[3] D. R. Mariani, W. van de Water, R. M. Koch, and T. Bergeman, Phys. Rev. Lett. **50**, 1261 (1983).

[4] P. Pillet, H. B. van Linden van den Heuvell, W. W. Smith, R. Kachru, N. H. Tran, and T. F. Gallagher, Phys. Rev. A **30**, 280 (1984).

[5] P. Fu, T. J. Scholz, J. M. Hettema, and T. F. Gallagher, Phys. Rev. Lett. **64**, 511 (1990).

[6] M. R. W. Bellerman, P. M. Koch, D. R. Mariani, and D. Richards, Bull. Am. Phys. Soc. **39**, 1120 (1994).

[7] M. R. W. Bellerman, P. M. Koch, D. R. Mariani, and D. Richards (private communication).

[8] M. J. Rakovic and S. I. Chu, Phys. Rev. A **50**, 5077 (1994).

[9] C. Y. Lee, J. M. Hettema, C. H. Cheng, C. W. S. Conover, and T. F. Gallagher, J. Phys. B (to be published).

[10] H. Kogelnik and T. Li, Proc. IEEE **54**, 1312 (1966).

[11] C. Y. Lee, Ph.D. thesis, University of Virginia (1994).

[12] C. R. Mahon, J. L. Dexter, P. Pillet, and T. F. Gallagher, Phys. Rev. A **44**, 1859 (1991).

[13] M. L. Zimmerman, M. G. Littman, M. M. Kash, and D. Kleppner, Phys. Rev. A **20**, 2251 (1979).

[14] D. Wintgen, Z. Phys. D **18**, 125 (1991).